International Journal of Power Electronics and Drive System (IJPEDS)
Vol. 10, No. 1, March 2019, pp. 10~18
ISSN: 2088-8694, DOI: 10.11591/ijpeds.v10.i1.pp10-18

A simple constant switching frequency of direct torque control of brushless DC motor

Yusnida Tarmizi[1], Auzani Jidin[2], Kasrul Abdul Karim[3], Tole Sutikno[4]
[1,2,3]Faculty of Electrical Engineering, Universiti Teknikal Malaysia Melaka, Malaysia
[1,2,3]Electrical Machine Design, Power Electronics and Drives Research Group, CeRIA, UTeM, Malaysia
[4]Department of Electrical Engineering, Universitas Ahmad Dahlan, Indonesia

Article Info

Article history:

Received Aug 9, 2018
Revised Nov 12, 2018
Accepted Dec 3, 2018

Keywords:

BLDC
CSF
DTC

ABSTRACT

This paper discusses about direct torque control of Brushless DC motor by injecting the triangular waveform and using PI controller in order to reduce the torque and obtain constant switching frequency. Brushless DC motor are widely used in applications which require wide range of speed and torque control because of robust, longer lifespan, faster torque response and able to operate at high speed. Unlike conventional three phase DTC of induction machine (IM), the proposed DTC approach introduces two phase conduction mode. Besides that, the magnitude flux is considered constant in which the results only gains from constant torque region. Thus, the flux control loop is eliminated while implement this scheme. Using the triangular waveform that will be compare with actual torque, the proper switching pattern can be selected to control the generated torque and reducing commutation torque ripple. The torque response depends on the speed of the stator flux linkage which is directly controlled by selecting appropriate voltage space vectors from a look-up table to make sure the torque error within the band. The validity of the proposed control scheme for constant switching frequency and reduce torque ripple are verified through simulation and experimental results.

Corresponding Author:

Kasrul Abdul Karim,
Faculty of Electrical Engineering,
Universiti Teknikal Malaysia Melaka,
Hang Tuah Jaya, 76100 Durian Tunggal, Melaka, Malaysia.
Email: kasrul@utem.edu.my

1. INTRODUCTION

The Brushlesss Direct Current (BLDC) motor become popular and gradually replacing conventional DC machine drives in many industrial applications such as appliances, automotive, consumer, aerospace, instrument and others. The BLDC motor is electrically commutated by power switches instead of brushes in order to improve the reliability and durability of the unit. For instance, the electrical commutation happened with permanent magnet rotor and stator coisl in a proper sequence. The force acting on the rotor causes it to rotate when the armature coils are switched electronically by transistor at the right fiels poles. The Hall effect sensors is used to detect the current commutation points that occur every 60 electrical degrees. Therefore, three sensors has been placed into the stator in the motor with 120 degree lag with respect to the other two sensors. These sensors are named as Hall A, Hall B and Hall C. Generally, whenever rotor magnetic poles pass near the hall-effect sensor, a high or low signal will be corresponded when the North or South Pole is passing near the sensors. Noted that, the North pole signal is indicates to '1' and the South Pole to '0'[1]. Unlike induction motor, BLDC operates in two-phase conduction mode which means only two phases conduct at any instant of time. The process occurs in order to control torque by keeping the stator flux linkage amplitude almost constant by eliminating the flux control. Since the flux control is constant, there are a few algorithms needed for the proposed control scheme. As conclusion, only torque is being control while

the stator flux linkage is kept constant on purpose. Furthermore, by using zero voltage vector suggested in [2], the electromagnetic torque will decrease which give some opportunity such as generating more frequent and larger spikes for the phase voltages. This effect will deteriorate the trajectory of the stator flux linkage locus.

The BLDC motor provide many advantages such as higher efficiency and reliability, have longer lifespan, robust, faster torque response, and able to operate at higher speed [3]. Moreover, their popularity is also assisted due to declining cost as well as increasing functionality. BLDC can be smaller and ligther as there were brushless type with the same power output to be used for application where space is limited. The BLDC has a non-sinusoidal back-EMF which is nearly trapezoidal or rectangular shape of waveform for stator phase current due to magnet displacement and concentrated winding. Therefore, particular control approach is required in order to develop constant mutual torque [4]. However, BLDC has a major drawback which during operation produce large torque ripple and variable inverter switching frequency. Despite machine structure, the input system due to switching techniques and phase current commutation that comes from power electronic side is the main reason for torque waveform becomes imperfection.

Over the past three decades, Direct Torque Control (DTC) schemes has been proposed by [5] for induction machine. Since the beginning, it has been developed and presented with simplicity, good performance and robustness [6]. It gained popularity among the researcher as it offers excellent dynamic performance which comparable to that obtained in the DC drives and robust to motor parameter. DTC of BLDC with non-sinusoidal back-EMF is proposed in [7], [8]. The stator flux and electromagnet torque were obtained from two-level and there-level hysteresis controller respectivey by comparing the stator flux linkage and estimated electromagnetic torque with their demands value. Therefore, to satisfy the flux and torque demands, the suitable voltage vector are selected from a look-up table either to increase or decrease the torque or the same time to either increase or decrease the stator flux. Other than that, a through investigation on the many switching technique in DTC, especially in reducing torque ripple and provide a constant switching frequency, before formulating the proposed controller strategy. Obviously, the used of space vector modulation (SVM) is consider as the most popular variations in DTC whether for induction motor (IM) and brushless DC motor (BLDC). However, this technique which normally referred to a DTC-SVM needs major modifications on the original DTC structure. Besides that, some other technique also has been proposed by researcher to improve the DTC performance while putting some efforts which retains the simple structure of DTC scheme. Because of that, the schemes require machine parameter in order to design the proper PI controllers. Recently, the use of multilevel inverter has gained much attention due to its advantages inproviding greater number of voltage vectors, lower switching loss and lower harmonics. Hypothetically, the greater the number of voltage vectors, the more option are given to select the most optimal voltage vectors in order to improve the DTC performance. However, the multilevel inverter may complicate the DTC structure and give some problems such as requirement of isolated DC voltages in CHMI, the inbalance neutral or capacitor's voltage in NPCMI. In the view of this scenario, this paper initially proposes using PI controller and injection triangular waveform in order to achieve torque ripple-free operation of BLDC motor.

2. BASIC STRUCTURE

2.1. Mathematical Modelling of BLDC Motor

A precise study of the BLDC operation is made in order to study and understand the dynamic behavior of the DTC drive. Modelling BLDC motor requires two equations which are electrical and mechanical equation. Brushless DC motor equation can be expressed as follows:

Electrical equation:

$$V_{kn}(t) = i_k R_k + L_k \frac{d_{i_k}}{dt}(t) + e_k(t) \quad (1)$$

$V_{kn}(t)$ = instantaneous of k – phase voltage
$i_k(t)$ = instantaneous of k – phase current
$e_k(t)$ = instantaneous of k – phase back-emf voltage
R_k = k – phase resistance
L_k = k-phase inductance

The model of armature winding for BLDC motor can be clearly expresses as follows based (1):

$$V_a = i_a R_a + L_a \frac{d_{i_a}}{dt} + e_a \quad (2)$$

$$V_b = i_b R_b + L_b \frac{d_{i_b}}{dt} + e_b \quad (3)$$

$$V_c = i_c R_c + L_c \frac{d_{i_c}}{dt} + e_c \quad (4)$$

Brushless DC motor equation with 120º conduction angle and trapezoidal back-EMF waveform can be expressesd as,

$$e_a(t) = K_{E_I}(\theta_e)\omega(t) \quad (5)$$

$$e_b(t) = K_{E_I}(\theta_e - \tfrac{2\pi}{3})\omega(t) \quad (6)$$

$$e_b(t) = K_{E_I}(\theta_e + \tfrac{2\pi}{3})\omega(t) \quad (7)$$

where,
K_{E_I} = back EMF constant of one phase
θ_e = electrical rotor angle
ω = rotor speed

Mechanical equation:

Next, mechanical equation where involve torque, angular velocity and friction of the rotor are shown. The total of torque that produced for each phase can be represented as below:

$$T_{emf}(t) = \sum_{k=a,b,c} T_{emf}\,(t) \quad (8)$$

$$T_{emf}(t) = i_k(t).K_{T,k}(\theta) \quad (9)$$

$$e_k(t) = k_{v,k}(\theta).\omega_e(t) \quad (10)$$

where, $k_{T,k}$ is the torque factor.

2.2. Direct Torque Control of BLDC Motor

The Figure 1 shows the structure of DTC of BLDC motor. The stator flux in the voltage vector look-up table is selected as -zero or constant while the torque error is selected based in difference of error level between the actual torque and the reference torque. The direct torque control of BLDC motor is explained in [9], for two phase conduction with only torque control loop.The selection of voltage vector is depends on the torque error which comes from the difference between estimated torque and reference torque. When the torque error touches the upper or lower hysteresis band, an appropriate voltage vector is selected whether to reduce or increase it respectively. Torque error status from comparators is required in order to determine the appropriate voltage vector where it can be '1' or '-1'. When torque status is '1' or positive, means that the torque error touches the upper hysteresis band and actual torque should decrease and thus voltage vector opposite to the direction of rotation of reference stator flux is chosen as shown in Figure 3 or else if the torque error status is '-1' or negative, this means that the torque error touches the lower hysteresis band and actual torque has to be decreased so the voltage space vector in the direction of rotation of the actual stator flux vector is selected. The selection of the respective voltage vector also depends on the sector given from sector 1 until sector 6 in which the rotor is present. Thus, the basis of this switching table is given as Table 1.

The Figure 2 shows the six nonzero voltage vectors ($\bar{V}_{S_1}$ - $\bar{V}_{S_6}$) that shape the axes of a hexagonal and feed electrical power to the load. The angle between any adjacent two non-zero voltage vectors or also known as active voltage vectors is 60 degrees, while two zero voltage vectors (non-active voltage vector) ($\bar{V}_{S_0}$ and $\bar{V}_{S_7}$) are at the origin and apply zero voltage to the load.

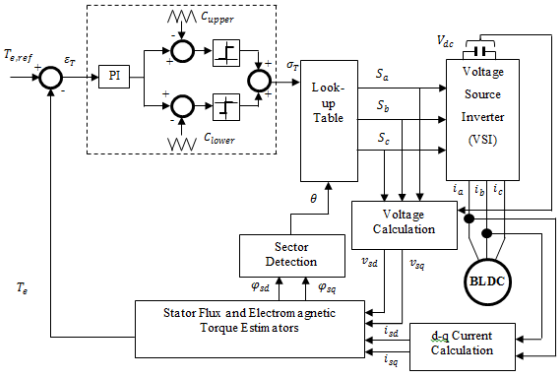

Figure 1. Structure of DTC of BLDC motor

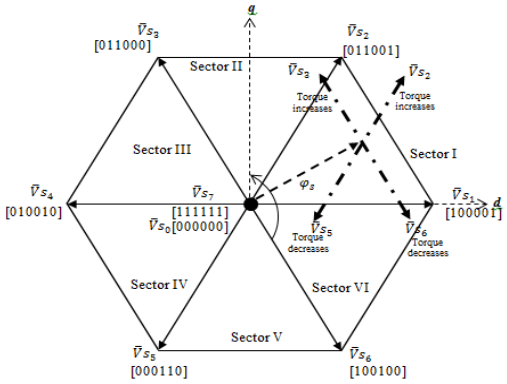

Figure 2. Selection of voltage space vectors to increase or decrease torque

The Table 1 shows the voltage vector selection for BLDC motor according to stator flux and torque errors. Noted that, only the yellow colour is used because the flux for BLDC motor is assumed as zero or constant.

Table 1. Voltage vector selection table

Flux	Torque	Sector					
		1	2	3	4	5	6
1	1	V1	V2	V3	V4	V5	V6
	-1	V6	V1	V2	V3	V4	V5
0	*1*	*V2*	*V3*	*V4*	*V5*	*V6*	*V1*
	-1	*V5*	*V6*	*V1*	*V2*	*V3*	*V4*
-1	1	V3	V4	V5	V6	V1	V2
	-1	V4	V2	V3	V4	V5	V6

2.3. Injection of Carrier Waveform

The torque error is the input for look-up table as the results from difference between carrier waveform and actual torque. Injection of carrier waveform technique is conceptually easy to understand. The mathematical concepts behind this technique reasoning are simple. This technique (injection carrier waveform) is implemented and explained in [10] for induction motor. A similar approach is used in this paper. In doing so, the triangular waveform frequency must set at high value in order to reduce output torque ripple hence faster torque response. For PI controller, it is necessary to make sure that the gain values of k_p and k_i are restricted so that the absolute slope of Tc not to exceed the absolute slope of the triangular (carrier) waveform. Figure 3 shows the typical waveform for constant frequency torque controller (CFTC).

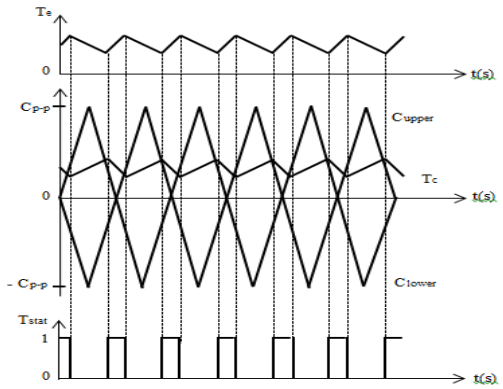

Figure 3. Typical waveform of the constnt frequency torque controller

3. MEASUREMENT SETUP

Table 2 shows Parameters of BLDC Motor. Figure 4 shows diagram for torque and constant switching frequency setup. Speed sensor (Hall Effect) will measure the speed rpm which will be shown by digital speed indicator. dSPACE 1104 is controller board that been used to transfer data from BLDC motor and allows the data to be present in oscilloscope and Control desk from computer. 15 V is supplied to the current sensor which function to sense the current value accurately for phase a and b in the BLDC motor as it is important to calculate the value of estimated torque. 100V – 150V is supplied to the BLDC motor from power supply.

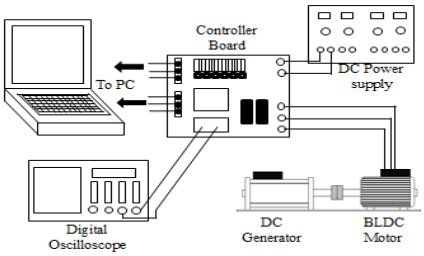

Figure 4. Schematic for experiment set up

Table 2. Parameters of BLDC motor

Baldor's BLDC Motor (25P002B002)	
Control System	
Torque Hysteresis Band	0.1 Nm
Flux Hysteresis Band	0.1 Wb
Sampling Time	50 µs
General Parameters	
Cont. Stall Torque Lb-In (N-M):	18.50 (2.10)
Cont. Stall Current:	1.5
Peak Torque Lb-In (N-m):	55.5 (6.3)
Electrical Parameters	
Torque Constant Lb-In/Amp (N-m/Amp):	15.50 (1.75)
Voltage constant v/r/s (V/KRPM):	150.000 (106.1)
Resistance	26.7
Inductance (mH)	106.3
Mechanical Parameter	
Inertia Lb-In-s2 (kg-cm^2):	0.0024 (2.72)
Speed at 320 Bus Volts (RPM):	1800
Pole pairs	2
Feedback Devise	
Hall Sensor	
Incremental Encoder	

4. SIMULATION RESULTS

In this experiment, three schemes were tested under three different speed operations, i.e. low speed, middle speed and high speed. The experiment for each scheme was performed using torque control loop, in which the angular velocity of BLDC motor was set at around the three levels of speed operations by applying appropriate load torque. The rest parameter control values for each scheme were given in Table 3.

Table 3. Parameter control for each scheme

	Control Schemes	
	(a) DTC	(b) CSF
Reference torque, T_{ref}	0.9 Nm	0.9 Nm
Sampling time, T_s	50 µs	50 µs
Torque hysteresis bandwidth, HB_T	0.09 Nm	-
Current hysteresis bandwidth, HB_i	0.0592 Nm	-
PI torque control:		
Proportional gain, K_{pT}	-	2.67
Integral gain, K_{iT}	-	50
Carrier frequency, f_{sw}	-	3125 Hz
Peak of carrier, V_{tri}	-	100

Figure 5 shows the experimental results of motor torque, torque error and *a*-phase current for each scheme, at low speed, medium speed and high speed. Figure 6 shows the zoomed image for presenting clearer results in highlighting the improvement/effect. It can be observes that the ripple sizes of torque in proposed CSF scheme are reduced compare to DTC scheme. The improvements obtained in the proposed CSF at the low-speed operation were also verified in the case of medium and high speed operations. Figure 5 (b) and Figure 6 (b) show the experimental results for the case of the medium-speed operation, while Figure 5 (c) and Figure 6 (c) shows the experimental results for the case of the high-speed operation. The types of waveforms obtained and torque reference applied in these figures are same as the case of low-speed operation. The only difirent is that the level of speed operation, which can be noticed by observing the cycle period of the current at the same time scale. Noted that, the greater number of cycle indicates higjer speed operations. Apparently, torque or current ripple is reduced for every level of speed operation, i.e. regardless of speed operations.

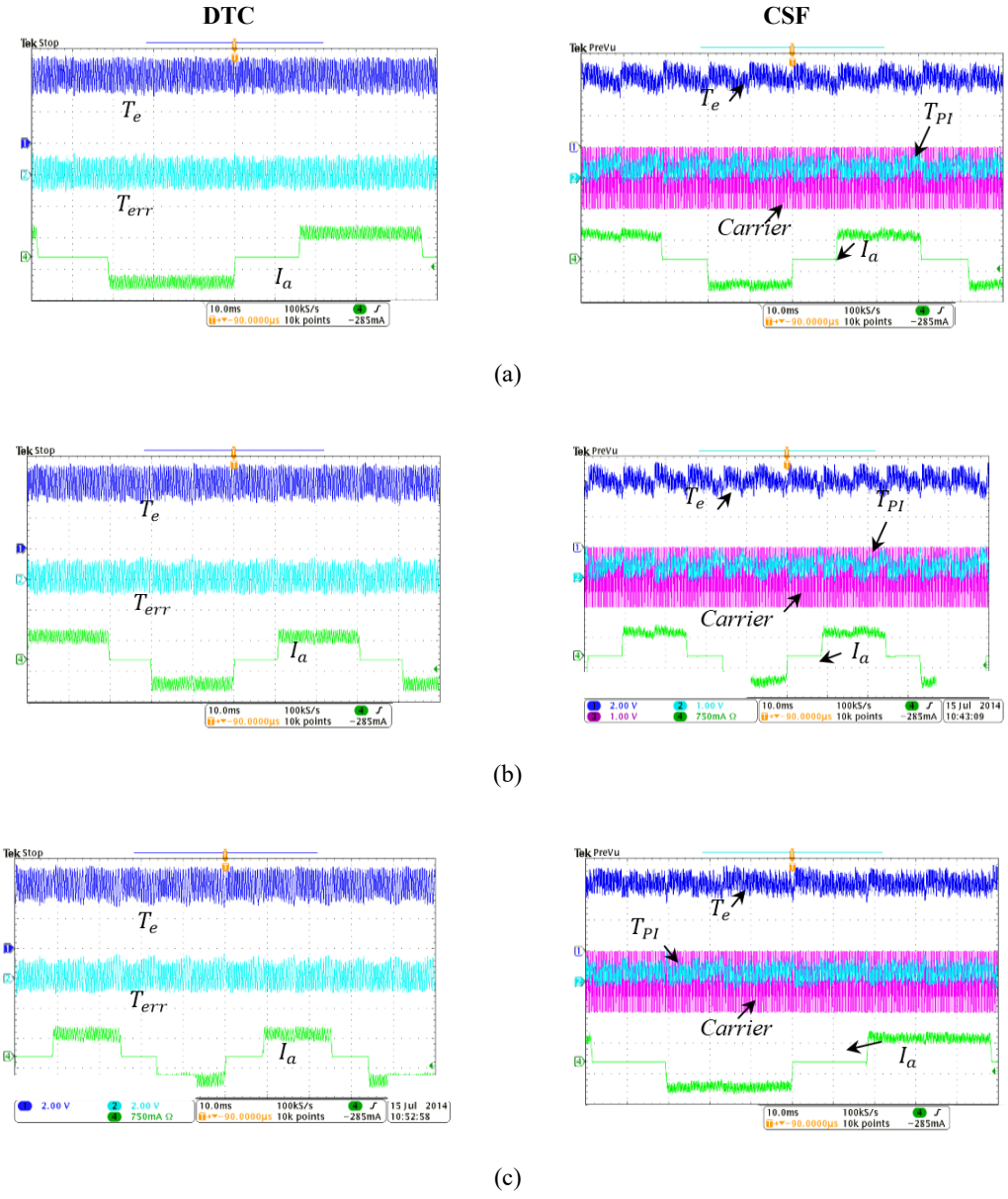

Figure 5. Experimental results of torque control for DTC and CSF at (a) low speed, (b) medium speed and (c) high speed operations

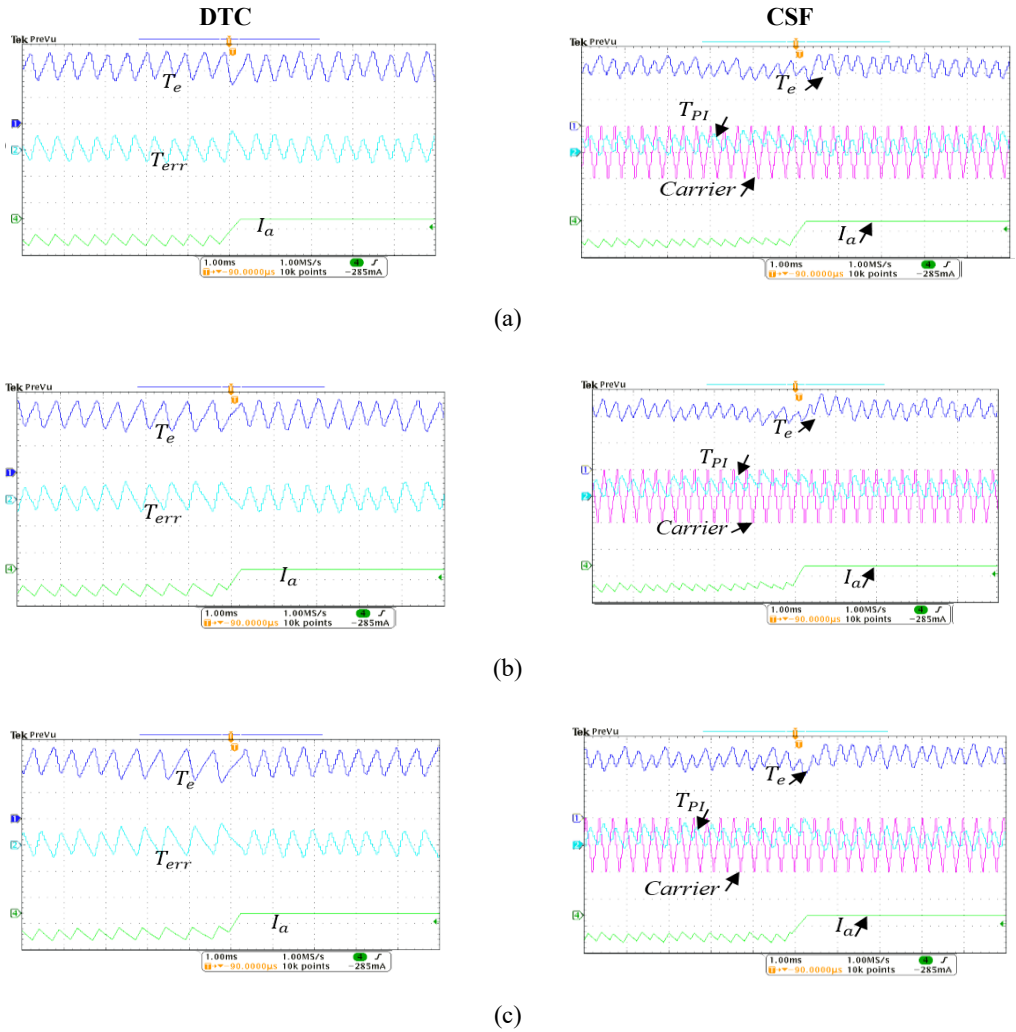

Figure 6. Experimental result of zoom-image for DTC and CSF at (a) low speed, (b) medium speed and (c) high speed operations

In order to determine the dominant switching frequency for each shemes, the frequency spectrum of a torque waveform at 0.9 Nm as mentioned in Table 3 was plotted as despicted in Figure 7. It can be clearly seen that the proposed CSF results in a dominant harmonic component as its carrier frequency, i.e. f_{sw} =3125 Hz. This indicates that the switching frequency of inverter is constant at the carrier frequency, while DTC exhibit scattered harmonic components due to hysteresis operation. Note that the scattered harmonic components show the switching frequencies based on hysteresis controller are unpredictable; that vary according to the operating conditions.

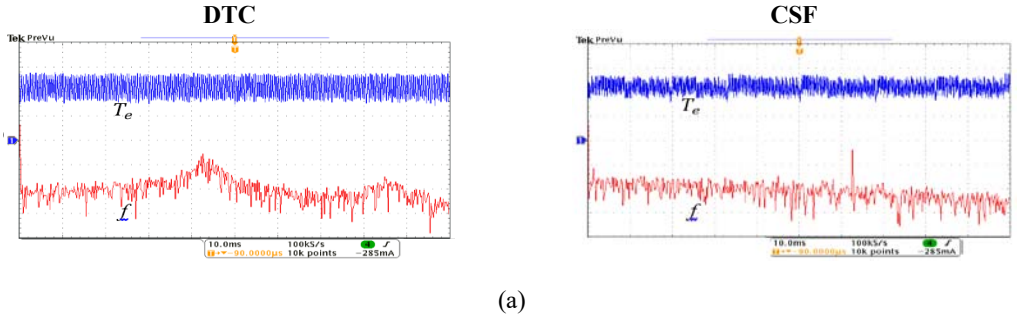

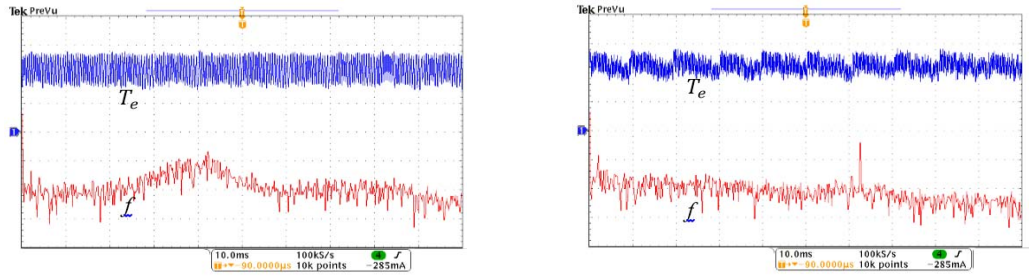

(b)

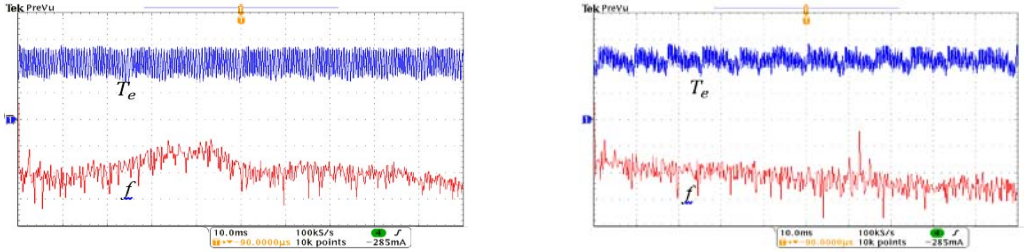

(c)

Figure 7. Frequency spectrum of torque waveform for DTC and CSF at (a) low speed, (b) medium speed and (c) high speed operations

5. CONCLUSION

In conclusion, the direct torque control drive has been implemented for Brushless DC Motor to reduce torque ripple and improve variable frequency by replacing the torque hysteresis controller with the Constant Switching Frequency (CSF) in the basic DTC scheme. In this research, the comparison of output torque and switching frequency between DTC hysteresis-based and DTC-CSF were experimented in several conditions (low, medium and high operation) of motor had been presented. Based on the results, it proven that at any condition, the CSF method can reduced torque ripple and provided a constant switching frequency for DTC drive. Finally, it can be concluded the DTC with CSF menthod was successfully implemented using BLDC motor.

ACKNOWLEDGEMENTS

The authors would like to thank Ministry of Education Malaysia, Universiti Teknikal Malaysia Melaka (UTeM) for providing the research grant PJP/2017/ FKE/HI12/S01538 and FRGS/2/2014/TK03/UTEM/03/2/ F00239.

REFERENCES

[1] M. Barcaro, "Performance Evaluation of an Integrat Ed Starter Alternator using an Interior Permanent Magnet Machine," *IET Electronic on Power Applied*, vol.4, pp.539-546, 2010.
[2] T. Yoon, "Magnetically Induced Vibration in a Permanent-Magnet Brushless DC Motor with Symmetric Pole-Slot Configuration," *IEEE Transactions on Magnetics*, vol. 41, pp. 2173-2179, 2005.
[3] Z. Q. Zhu and D. Howe, "Influence of Design Parameters on Cogging Torque in Permanent Magnet Machines," *IEEE Transaction Energy Conversion*, vol. 15, pp. 407–412, 2000.
[4] J. Hur and B. W. Kim, "Rotor Shape Design of an Interior PM type BLDC Motor for Improving Mechanical Vibration and EMI Characteristics," *Journal of Electrical Engineering and Technology*, vol. 5, pp. 462–467, 2010.
[5] Z. Q. Zhu, M. L. Mohd Jamil, and L. J. Wu, "Influence of Slot and Pole Number Combinations on Unbalanced Magnetic Force in Permanent Magnet Machines," *Energy Conversion Congress and Exposition (ECCE), 2011 IEEE*, pp. 1-8, 2011.
[6] S. M. JafariShiadeh, M. Ardebili, "Three-Dimensional Finite-Element-Model Investigation of Axial-Flux PM BLDC Machines with Similar Pole and Slot Combination for Electric Vehicles," *Power and Energy Conference at Illinois (PECI), 2015 IEEE*, pp. 1-4, 2015.
[7] K. O. Sung, C. S. Hong, and P. Han, "Flux Fluctuations in Rotor Core According to PoleSlot Combination," *2012 IEEE Vehicle Power and Propulsion Conference*, pp. 1045-1047, 2012.

[8] L. Ma, M. Sanada, S. Morimoto and Y. Takeda, "Prediction of Iron loss in rotating machines with rotational loss include," *IEEE Transactions on Magnetics*, vol. 39, pp. 2036-204, 2003.
[9] Salih Baris Ozturk, H. A. Toliyat, "Direct Torque Control of Brushless DC Motor with Non-Sinusoidal Back-EMF", *Electric Machines & Drives Conference (IEMDC),* 2007
[10] Jidin, A., Idris, N. R. N., Yatim, A. H. M., Sutikno, T. and Elbuluk, M. E., "Simple Dynamic Overmodulation Strategy for Fast Torque Control in DTC of Induction Machines with Constant-Switching-Frequency Controller", *IEEE Transactions Industry Application,* vol. 47, pp. 2283-2291, 2010.
[11] V. Mostafa, N. Arne, N. Robert, D. L. Robert and R. Terje, "Influence of Pole and Slot Combinations on Magnetic Forces and Vibration in Low-Speed PM Wind Generators," *IEEE Transactions on Magnetics*, vol. 50, pp. 1-11, 2014.
[12] P. M. Lindh, H. K. Jussila, M. Niemela, A. Parviainen, and J. Pyrhonen, "Comparison of concentrated winding permanent magnet motors with embedded and surface-mounted rotor magnets," *IEEE Transactions on Magnetics*, vol. 45, no. 5, pp. 2085–2089, 2009.
[13] J. Yang, G. Liu, W. Zhao, Q. Chen, Y. Jiang, L. Sun, *et al.*, "Quantitative comparison for fractional-slot concentrated-winding configurations of permanent-magnet vernier machines," *IEEE Transactions on Magnetics*, vol. 49, pp. 3826–3829, 2013.
[14] S. U. Chung, J. M. Kim, D. H. Koo, B. C. Woo, D. K. Hong, and J. Y. Lee, "Fractional slot concentrated winding permanent magnet synchronous machine with consequent pole rotor for low speed direct drive," *IEEE Transactions on Magnetics* vol. 48, pp. 2965–2968, 2012.
[15] A. S. Abdel-Khalik, S. Ahmed, A. Massoud, and A. Elserougi, "An improved performance direct-drive permanent magnet wind generator using a novel single layer winding layout," *IEEE Transactions on Magnetics*, vol. 49, pp. 5124–5134, 2013.
[16] S. Lee, Y. J. Kim, and S. Y. Jung, "Numerical investigation on torque harmonics reduction of interior PM synchronous motor with concentrated winding," *IEEE Transactions on Magnetics*, vol. 48, pp. 927–930, 2012.
[17] S. K. Lee, G. S. Kang, and J. Hur, "Finite Element Computation of Magnetic Vibration Sources in 100 kW two Fractional-slot Interior Permanent Magnet Machines for Ship," *IEEE Transactions on Magnetics*, vol. 48, pp. 867–870, 2012.
[18] A. M. EL-Refaie, "Fractional-slot Concentrated-windings Synchronous Permanent Magnet Machines: Opportunities and challenges," *IEEE Transactions on Industrial Electronic*, vol. 57, pp. 107–121, 2010.
[19] A. M. EL-Refaie, "Fractional-slot concentrated-windings: A paradigm shift in electrical machines," in *Proceeding IEEE WEMDCD*, *Mar. 2013*, pp. 24–32, 2013.
[20] F. Libert and J. Soulard, "Investigation on Pole-slot Combinations for Permanent-Magnet Machines with Concentrated Windings," in *Proceeding ICEM*, 2004, pp. 1–6, 2004.
[21] Y. S. Chen, Z. Q. Zhu, and D. Howe, "Vibration of PM Brushless Machines having a Fractional Number of Slots Per Pole," *IEEE Transactions on Magnetics*, vol. 42, pp. 3395–3397, 2006.
[22] G. Dajaku and D. Gerling, "Magnetic radial force density of the PM machine with 12-teeth/10-poles winding topology," in *Proceeding IEEE IEMDC, May 2009*, pp. 1715–1720, 2009.
[23] N. Bianchi, S. Bolognani, M. D. Pre, and G. Grezzani, "Design considerations for fractional-slot winding configurations of synchronous machines," *IEEE Transactions on Industrial Application*, vol. 42, pp. 997–1006, 2006.
[24] R. N. Firdaus, S. Farina, R. Suhairi, K. A. Karim, F. Azhar, A. Khamis and M. Norhisam, "Improvement of Torque Density Spoke Type BLDC Motor Using New Hollow Rotor Topology," *International Review of Electrical Engineering (I.R.E.E.),* vol. 12, pp. 19-25, 2017.
[25] R. N. Firdaus, S. Farina, R. Suhairi, K. A. Karim, J. Auzani, S. Tole and M. Norhisam, "Design of Hollow-Rotor Brushless DC Motor," *International Journal of Power Electronics and Drive System (IJPEDS)*, Vol. 7, pp. 387-396, 2016.
[26] S. Ohira, N. hasegawa, I. Miki, D. Matsuhashi, and T. Okitsu, "Torque Characteristics of IPMSM with Spoke and Axial Type Magnets," *SPEEDAM 2012 - 21st International Symposium on Power Electronics, Electrical Drives, Automation and Motion*, pp. 818–821, 2012.
[27] H. Nam, K. H. Ha, J. I. Lee, J. P. Hong and G. H. Kang, "A study on iron loss analysis method considering the harmonics of the flux density waveform using iron loss curves tested on Epstein samples," *IEEE Transactions on Magnetics*, vol. 39, pp. l472-1475, 2003.